

CONTRIBUTIONS TO THE NEARBY STARS (NSTARS) PROJECT: SPECTROSCOPY OF STARS EARLIER THAN M0 WITHIN 40 pc—THE SOUTHERN SAMPLE

R. O. GRAY

Department of Physics and Astronomy, Appalachian State University, Boone, NC 28608; grayro@appstate.edu

C. J. CORBALLY

Vatican Observatory Research Group, Steward Observatory, Tucson, AZ 85721-0065; corbally@as.arizona.edu

R. F. GARRISON

David Dunlap Observatory, P.O. Box 360, Station A, Richmond Hill, ON L4C 4Y6, Canada; garrison@astro.utoronto.ca

M. T. McFADDEN, E. J. BUBAR,¹ AND C. E. MCGAHEE

Department of Physics and Astronomy, Appalachian State University, Boone, NC 28608

AND

A. A. O'DONOGHUE AND E. R. KNOX

Department of Physics, St. Lawrence University, Canton, NY 13617

Received 2006 February 1; accepted 2006 March 27

ABSTRACT

We are obtaining spectra, spectral types, and basic physical parameters for the nearly 3600 dwarf and giant stars earlier than M0 in the *Hipparcos* catalog within 40 pc of the Sun. Here we report on results for 1676 stars in the southern hemisphere observed at Cerro Tololo Inter-American Observatory and Steward Observatory. These results include new, precise, homogeneous spectral types, basic physical parameters (including the effective temperature, surface gravity, and metallicity [M/H]), and measures of the chromospheric activity of our program stars. We include notes on astrophysically interesting stars in this sample, the metallicity distribution of the solar neighborhood, and a table of solar analogs. We also demonstrate that the bimodal nature of the distribution of the chromospheric activity parameter $\log R'_{\text{HK}}$ depends strongly on the metallicity, and we explore the nature of the “low-metallicity” chromospherically active K-type dwarfs.

Key words: solar neighborhood — stars: abundances — stars: activity — stars: fundamental parameters — stars: late-type — stars: statistics

Online material: machine-readable tables

1. INTRODUCTION

This is the second in a series of three papers that present results of a joint study of the nearby solar-type stars under the aegis of the NASA/JPL Nearby Stars (NSTars)/*Space Interferometry Mission* Preparatory Science Program. The goal of this project is to obtain spectroscopic observations of all 3600 main-sequence and giant stars with spectral types earlier than M0 in the *Hipparcos* catalog (Perryman et al. 1997) within 40 pc of the Sun. We have obtained blue-violet classification-resolution (1.5–3.6 Å) spectra for all of these stars to date. These spectra are being used to obtain homogeneous, precise, MK spectral types. In addition, these spectra are being used in conjunction with synthetic spectra and existing intermediate-band Strömgren *uvby* and broadband *VRI* photometry to derive the basic astrophysical parameters (the effective temperature, gravity, and overall metal abundance [M/H]) for many of these stars. We are also using these spectra, which include the Ca II K and H lines, to obtain measures of the chromospheric activity of the program stars on the Mount Wilson system. The purpose of this project is to provide data that will permit an efficient choice of targets for both the *Space Interferometry Mission* and the *Terrestrial Planet Finder (TPF)*. In addition, combination of these new data with existing kinematic data should enable the identification and characterization of stellar subpopulations within the solar neighborhood.

We report in this paper on southern hemisphere stars for which observations have been carried out on the 1.5 m telescope at Cerro Tololo Inter-American Observatory (CTIO) and the 2.3 m Bok telescope at Steward Observatory (SO), which is situated on Kitt Peak. Other observations for this project have been carried out on the 0.8 m telescope of the Dark Sky Observatory (DSO) and the 1.8 m telescope at the David Dunlap Observatory. Observations of 664 stars carried out at DSO were the subject of the first paper of this series (Gray et al. 2003, hereafter Paper I). The remaining stars in our sample will be reported on in the third paper of this series (R. O. Gray et al. 2006, in preparation).

2. OBSERVATIONS AND CALIBRATION

The observations reported in this paper were made with the 1.5 m telescope at CTIO and the 2.3 m Bok telescope at SO. The CTIO observations were carried out using the Loral 1200 × 800 CCD on the Cassegrain spectrograph. Grating 58 was used in the second order with the CuSO₄ order-blocking filter and a slit size of 86 μm to give a nominal resolution of 2.6 Å (2 pixels) with a wavelength range of 3800–5150 Å. However, in practice, the actual resolution of these spectra is closer to 3.5 Å. These spectra were reduced using standard methods with IRAF.² The Loral CCD on the CTIO 1.5 m Cassegrain spectrograph has a number of blemishes that affected these spectra. In particular, one blemish

¹ Department of Physics and Astronomy, Clemson University, Clemson, SC 29634.

² IRAF is distributed by the National Optical Astronomy Observatory, which is operated by the Association of Universities for Research in Astronomy, Inc., under cooperative agreement with the National Science Foundation.

TABLE 1
OBSERVING LOG

Telescope	Dates
SO Bok 2.3 m.....	2000 Dec 21–23
CTIO 1.5 m.....	2001 Feb 4–9
SO Bok 2.3 m.....	2001 Mar 11–12
SO Bok 2.3 m.....	2001 Apr 8–9
SO Bok 2.3 m.....	2001 Jun 1–5
CTIO 1.5 m.....	2001 Aug 2–9
SO Bok 2.3 m.....	2001 Sep 8–10
SO Bok 2.3 m.....	2001 Nov 24–27
SO Bok 2.3 m.....	2001 Jan 1–2
SO Bok 2.3 m.....	2002 Jun 16–19
CTIO 1.5 m.....	2002 Jun 23–27
CTIO 1.5 m.....	2002 Dec 10–15
SO Bok 2.3 m.....	2003 Mar 11–13

affected the 4058–4069 Å region of these spectra; we carefully positioned the spectra so that this blemish did not affect the important Sr II λ 4077 line used in luminosity classification. Another blemish affected about 50% of the CTIO spectra, causing a distortion in the violet half of the G band. In total, we had four observing runs at CTIO, each lasting five-to-seven nights. Table 1 presents a log of these observing runs.

The SO observations were carried out using the Boller & Chivens spectrograph with the ccd20 CCD (1200 × 800 pixels) on the Bok 2.3 m telescope. The spectrograph was used with the 600 grooves mm⁻¹ red-blazed grating in the second order, the Schott 8612 order-blocking filter, and a slit size of 2"5 to give a resolution of 2.6 Å and a wavelength range of 3800–4960 Å. These spectra were likewise reduced using standard methods with IRAF. We had nine observing runs on the 2.3 m Bok telescope (see Table 1).

For stars with spectral types of G8 and earlier, the CTIO and SO spectra were rectified using an X Window System program, xmk19, written by one of us (R. O. G.), and were used in that format for both spectral classification and the determination of the basic physical parameters.

However, for the late-type stars (G8 and later) rectification is problematic, as no useful “continuum” points can be identified. For that reason, we have attempted to flux-calibrate these spectra even though they were obtained with a narrow slit. For this purpose, we regularly obtained spectra of a number of spectrophotometric standard stars (Hamuy et al. 1992) during the observing runs at both CTIO and SO. These standard observations have been used to remove approximately the effects of atmospheric extinction and to calibrate the spectrograph throughput as a function of wavelength. Except for observations made at high air masses, this procedure yields calibrations of *relative* fluxes with accuracies on the order of ±10%. We require greater accuracies, however, for the determination of the basic physical parameters, and so we have applied the technique of “photometrically correcting” these fluxes using Strömgren photometry (taken from the General Catalog of Photometric Data by Mermilliod et al. 1997). This technique was described in detail in Paper I. However, because these spectra span only two Strömgren bands (as opposed to the three bands employed in Paper I), an additional flux correction procedure was employed during the analysis to give the basic physical parameters (see below).

All of the spectra obtained for this paper are available on the project’s Web site.³ The rectified spectra found on that Web site

have an extension of “.rec”. Spectra that have been flux-calibrated but not photometrically corrected are normalized to unity at a common point (4503 Å) and have an extension of “.nor,” whereas photometrically corrected spectra are available in a normalized format (.nfx) and in terms of absolute fluxes (.flx) in units of ergs s⁻¹ cm⁻² Å⁻¹. Dates and times of observation and other information can be found in the “footers” of these spectra.

3. SPECTRAL CLASSIFICATION

The stars in this paper were classified on the MK system by direct visual comparison on the computer screen with MK standard stars selected from the list of “Anchor Points of the MK System” (Garrison 1994), the Perkins catalog (Keenan & McNeil 1989), and, for the late K- and early M-type dwarfs, Henry et al. (2002). Spectra of an extensive set of relevant standards were obtained on each telescope. A list of the standards used (and the actual spectra) can be found on the project Web site.

Paper I described the techniques we used to carry out the spectral classifications and how we ensured the homogeneity of our spectral types, which we derived from spectra obtained on four different spectrographs. In short, this homogeneity is maintained by significant overlaps between the samples observed with the four telescopes employed by this project, as well as having a number of MK standards in common between the different samples. Out of the 1676 stars reported in this paper, 78 stars were observed at both CTIO and SO. Spectral types were assigned independently for the two groups of stars. For the 78 stars in common, we find the following systematic difference in the spectral types:

$$ST_{CTIO} - ST_{SO} = 0.19 \pm 0.50,$$

and thus the CTIO spectral types are systematically later than the SO spectral types by 0.2 spectral subclasses, with a scatter (one point) of one-half a spectral subclass (note, a subclass is the difference, e.g., between a K0 and a K1 star). For this comparison, we used the numbering system of Keenan (1984) to convert spectral types into numerical codes. We note that this very small systematic difference in the spectral types indicates a high degree of consistency between the northern and southern sets of MK standards chosen for this work.

Our spectral types are multidimensional, as they include not only temperature and luminosity types but also indices indicating abundance peculiarities and the degree of chromospheric activity.

As described in Paper I, chromospheric activity is evident in our spectra through emission reversals in the cores of the Ca II K and H lines and, in more extreme cases, infilling and emission in the hydrogen lines. We continue the use of the spectral classification notation we introduced in Paper I to indicate increasing levels of chromospheric activity evidenced by these emission features: (k), k, ke, and kee. In the first two cases, infilling is seen only in the K and H lines; in the last two, infilling and emission can be seen in the Balmer lines as well, especially at H β . Because chromospheric emission is time-variable, these activity classes are necessarily time-dependent. We have therefore noted the observation date in the notes to the machine-readable version of Table 2 for those stars that have been designated as either “ke” or “kee.”

Spectral types for the stars analyzed in this paper can be found in Table 2. Figure 1 shows a classical H-R diagram (M_V vs. spectral type) for the stars in this paper and Paper I. One of the reasons why spectral types are valuable to this project is that they enable us to refine the stellar census in the solar neighborhood. Note

³ See <http://stellar.phys.appstate.edu>.

TABLE 2
SPECTRAL TYPES, BASIC PHYSICAL PARAMETERS, AND CHROMOSPHERIC INDICES

HIP	HD	SpT	N1	T_{eff}	$\log g$	ξ_t	[M/H]	N2	S_{MW}	$\log(R'_{\text{HK}})$	AC	N3	Obs
57.....	224789	K1 V	...	4999	4.48	1.0	-0.17	...	0.377	-4.568	A	...	CTIO
194.....	225003	F1 V	...	7043	4.07	2.0	-0.12	CTIO
296.....	225118	G8.5 V	...	5420	4.43	1.0	0.14	...	0.325	-4.570	A	...	SO
436.....	55	K4.5 V	0.338	-4.901	I	...	CTIO
522.....	142	F7 V	...	6257	3.99	2.7	-0.18	...	0.171	-4.853	I	...	CTIO
560.....	203	F3 Vn	...	6715	3.85	1.1	-0.19	*	SO

NOTES.—Table 2 is published in its entirety in the electronic edition of the *Astronomical Journal*. A portion is shown here for guidance regarding its form and content. See also § 6 for notes on astrophysically interesting stars. The column headings have the following meanings: HIP stands for the designation in the *Hipparcos* catalog (Perryman et al. 1997). HD stands for the HD designation. SpT stands for the spectral type—note that some long spectral types are contained in the notes. An asterisk in column N1 refers to a note on the spectral type. Columns T_{eff} , $\log g$, ξ_t , and [M/H] refer to the basic physical parameters—the effective temperature (kelvins), the logarithm of the surface gravity (cm s^{-2}), the microturbulent velocity in kilometers per second, and the overall metal abundance on a logarithmic scale, where [M/H] = 0.0 refers to solar metallicity. An asterisk in column N2 refers to a note on the fitting process; a K in this column indicates that the method used to determine the basic physical parameters was that adopted for the G and K giants. The S_{MW} column is the chromospheric activity index on the Mount Wilson system. The $\log R'_{\text{HK}}$ column is a measure of the chromospheric flux in the Ca II K and H lines. The AC column indicates the chromospheric activity class—VI for very inactive, I for inactive, A for active, and VA for very active. An asterisk in column N3 refers to a note on chromospheric activity. The Obs column indicates the source of the spectrum—CTIO for the 1.5 m Cassegrain spectrograph at Cerro Tololo Inter-American Observatory and SO for the Cassegrain spectrograph on the Bok 2.3 m telescope of Steward Observatory.

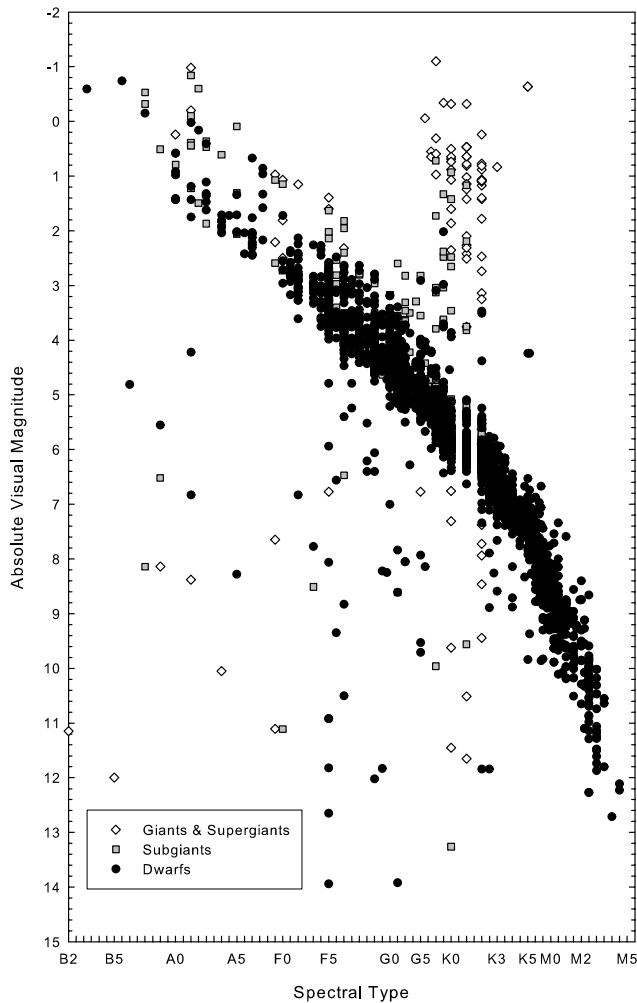


FIG. 1.—Observational H-R diagram formed from the spectral types of the 1676 stars reported in this paper and the 664 stars reported in Paper I. The absolute magnitudes, M_v , are calculated using *Hipparcos* (Perryman et al. 1997) parallaxes. The stars scattering below the main sequence in this figure all have large parallax errors and are listed in the notes to Table 2. These stars are all evidently more distant than 40 pc.

the stars in Figure 1 that scatter below the main sequence (white dwarfs are not plotted in this diagram). These stars, without exception, have *Hipparcos* (Perryman et al. 1997) parallaxes that place them within 40 pc but have large parallax errors, mostly due to binarity. These stars are indicated in the notes to Table 2. Note as well in Figure 1 a group of “dwarf stars” that lie above the main sequence (too far, in most cases, to be explained by binarity) and overlap the subgiant branch. These are an interesting and diverse group of stars. Most (HIP 3185, 14086, 18432, 46404, and 110618) are high-velocity, metal-weak stars (for which the luminosity class is notoriously difficult to determine). All of these stars have V components of their heliocentric space velocities $< -50 \text{ km s}^{-1}$ and thus are probably thick disk or halo stars and are most likely evolved. Two others are RS CVn binaries (HIP 16846 and HIP 84586 = HD 155555). HD 155555 is probably a pre-main-sequence (PMS) binary. Finally, one other star, HIP 117815, is a W UMa eclipsing binary.

Spectral types also provide beginning values for our determination of the basic physical parameters and provide a check on the derived physical parameters. But, most importantly, spectral types place a star within the context of a broad population of stars and enable us to pick out peculiar and astrophysically interesting stars.

4. BASIC PHYSICAL PARAMETERS

An important goal of this project is to determine the basic physical parameters—the effective temperature, the surface gravity, and the overall metallicity—for as many of our program stars as possible.

4.1. The Determination of the Basic Physical Parameters

We described in Paper I the technique that we use to determine the basic physical parameters for our program stars, and we refer the reader to that paper for the details. In summary, we determine the basic physical parameters by carrying out a simultaneous fit, using a variant of the multidimensional downhill simplex method (Press et al. 1992), between (1) the observed spectrum and a library of synthetic spectra and (2) observed fluxes from Strömgren *uvby* and Johnson-Cousins *VRI* photometry (taken from Merrill et al. 1997) and theoretical fluxes based on Kurucz (1993) ATLAS9 stellar atmosphere models (computed without convective overshoot). The library of synthetic spectra was calculated with the stellar spectral synthesis code SPECTRUM (Gray

& Corbally 1994)⁴ using ATLAS9 models. A graphics program, xfit21, written by one of us (R. O. G.), is used to set the initial parameters, which are then polished by the simplex engine. This graphical front end allows us to confirm that the simplex engine has indeed found the optimal global solution, and it also allows us to tweak that solution if necessary. The program xfit21 allows the user to apply rotational broadening when necessary and also to deredden the observed fluxes. However, since all of our stars are within 40 pc we have assumed the reddening for our stars to be zero.

As detailed in Paper I, for certain spectral types it was necessary to constrain one or more of the physical parameters in order to achieve reasonable solutions. This was especially the case for late-G and K dwarfs and giants. For the late-G and K dwarfs, neither our spectra nor the photometry strongly constrain the surface gravity. For these stars we have therefore constrained $\log g$ to the value implied by the *Hipparcos* parallax and the mass-luminosity relationship (Gorda & Svechnikov 1998). We have further constrained the microturbulent velocity ξ_t to be 1.0 km s^{-1} . However, we encountered an additional difficulty with the SO and CTIO spectra. Because these spectra have a shorter spectral range than the DSO 3.6 Å spectra used in Paper I for the late-G and K dwarfs and thus span only two Strömgren bands (v and b) instead of three, only a linear instead of a second-order spline could be used to apply the photometric correction. In addition, a significant number of the SO spectra were obtained at quite high air masses, and thus, the flux calibration for those spectra is quite unreliable. Because the accuracy of the flux calibration of the observed spectrum is of some importance in obtaining a reliable fit to the basic physical parameters for the late-type stars, we adopted the following procedure to overcome this difficulty, made possible by the xfit21 program. Having first constrained the gravity to the value implied by the mass-luminosity relation and the *Hipparcos* parallax and fixed ξ_t at 1.0 km s^{-1} , we set $[\text{M}/\text{H}] = 0.0$ and then adjusted the effective temperature to minimize the residuals between the photometric and theoretical fluxes. We then visually adjusted $[\text{M}/\text{H}]$ to match the line strengths in the observed and synthetic spectra and then iterated until the match was satisfactory. At this point, if the photometric correction of the observed spectral fluxes was satisfactory, the residuals between the observed and synthetic spectrum would be flat. If, however, the photometric correction was not satisfactory, these residuals might display a slope or a shallow curve as a function of the wavelength. If such was the case, the synthetic spectrum was used as a template to correct the fluxes in the observed spectrum. The simplex engine was then allowed to polish the final solution. While this correction procedure could be iterated, in practice we found that one application of this procedure gave a satisfactory fit to the basic physical parameters. Illustrations of typical simplex solutions may be found in Paper I.

Effective temperature determinations for the stars in common between SO and CTIO give us an excellent opportunity to test whether this modified method introduces any systematic error into the determination of the basic physical parameters. The reason for this is that most of these stars were obtained at high air mass from SO but were observed nearly overhead from CTIO. For the 56 dwarf stars in common between SO and CTIO with basic physical parameters, we find the following systematic difference in the effective temperatures:

$$T_{\text{CTIO}} - T_{\text{SO}} = 0 \pm 40 \text{ K},$$

where the uncertainty is for a single point. This also gives a good estimate for the internal error in the effective temperatures; the above comparison suggests that the internal precision in the temperature determinations is on the order of $\pm 30 \text{ K}$. For those dwarfs with $V - K$ photometry we may also compare our temperature scale with that of the “infrared flux” method (IRFM; Blackwell & Lynas-Gray 1994), which is essentially independent of theoretical models (see also Paper I). We find

$$\begin{aligned} T_{\text{CTIO}} - T_{\text{IRFM}} &= -4 \pm 16 \text{ K} \quad (29 \text{ stars}), \\ T_{\text{SO}} - T_{\text{IRFM}} &= 32 \pm 29 \text{ K} \quad (12 \text{ stars}), \end{aligned}$$

and, from Paper I,

$$T_{\text{DSO}} - T_{\text{IRFM}} = 28 \pm 17 \text{ K} \quad (50 \text{ stars}),$$

where the error displayed in all three cases is the error in the determination of the zero-point difference and not the scatter around the IRFM relationship. Combining the CTIO and the SO data sets, the scatter around the IRFM relation is $\pm 90 \text{ K}$, some of which is due to errors in the $V - K$ photometry (a change of 0.04 in $V - K$ at $V - K = 2.00$ results in a temperature change of 50 K). A plot of the residuals with respect to the IRFM relation shows no trend with effective temperature over the range 4600 – 8000 K . All three data sets show acceptably small and statistically indistinguishable zero-point differences with the IRFM method.

There are now a number of spectroscopic studies in the literature dealing with nearby stars with which we may profitably compare our temperature scale. Allende Prieto et al. (2004) used high-resolution spectroscopy to study the stars with $M_V < 6.5$ within 14.5 pc of the Sun. They base their temperatures on the calibrations of Alonso et al. (1996, 1999), who in turn derived their calibrations of $B - V$ and Strömgren photometry from the IRFM method. Our temperatures compare well with theirs, except for a slight trend in the residuals that amounts to our temperatures being about 50 K cooler than theirs at 5000 K and 120 K hotter at 6000 K . Once this trend is removed, the temperatures agree to within $\pm 70 \text{ K}$. The origin of this trend is not clear. Luck & Heiter (2005) have studied the stars with $M_V < 7.5$ within 15 pc of the Sun, but, unlike Allende Prieto et al., their atmospheric parameters were determined by requiring the abundance of iron to be independent of the excitation energy simultaneously with requiring that Fe I and Fe II give identical iron abundances. Our temperatures compare quite favorably with theirs, with a zero-point offset of 89 K (our temperatures are cooler) and a scatter of $\pm 108 \text{ K}$ but no trend in the residuals. Finally, Valenti & Fischer (2005) have studied 1040 nearby F-, G-, and K-type stars that have been observed in the Keck, Lick, and AAT planet search programs. They have used high-resolution spectra and a pipeline multivariate method to determine the basic physical parameters of these stars. Our temperature scales are virtually identical for the F- and G-type stars, but cooler than $T_{\text{eff}} = 5200 \text{ K}$ their temperatures begin to systematically deviate from ours (our temperatures are cooler), with the mean deviation approaching 100 K at 4800 K . For stars with effective temperatures greater than 5200 K , the scatter in the comparison of our temperatures with those of Valenti & Fischer is only $\pm 81 \text{ K}$, with a zero-point difference of 14 K (our temperatures are cooler).

In Paper I we adjusted the zero points of our $[\text{M}/\text{H}]$ determinations using well-studied stars in the Cayrel de Strobel et al. (2001) $[\text{Fe}/\text{H}]$ catalog, and we have done the same in this paper. Table 3 lists these zero-point corrections, which are generally

⁴ See <http://www.phys.appstate.edu/spectrum/spectrum.html>.

TABLE 3
ZERO-POINT CORRECTIONS TO $[M/H]$ SCALE

Stellar Type	CTIO	SO
F and G dwarfs.....	+0.02	+0.04
G and K dwarfs.....	+0.07	+0.07
G and K giants.....	+0.08	+0.06

quite small and similar in magnitude to those found in Paper I, with the exception of the K giants (see below).

It is of interest to compare the $[M/H]$ scales for the CTIO and SO spectra. We find, for the 56 stars in common,

$$[M/H]_{\text{CTIO}} - [M/H]_{\text{SO}} = 0.00 \pm 0.08,$$

where the quoted error is for a single point. Of course, the negligible zero-point difference is not surprising, as these metallicities include the zero-point corrections of Table 3, but the quoted error can be used to estimate the internal precision of the $[M/H]$ determinations. This is evidently on the order of ± 0.06 dex. Once the zero points have been applied (the $[M/H]$ values in Table 2 include these zero-point adjustments), the agreement with mean values in the $[Fe/H]$ catalog is excellent, with a scatter of ± 0.09 dex. Comparing the $[M/H]$ values in Table 2 with the Valenti & Fischer (2005) sample, however, we find an additional zero-point difference of 0.07 dex (our values are more negative) but a scatter of only ± 0.09 dex.

The method of determining the basic physical parameters for late G and K giants was essentially the same as that described in Paper I, although our improved method of applying a flux template at the midpoint of the fitting process (described above) appears to have significantly improved the quality of the fit for the K giants. Indeed, the zero-point correction for the K giant $[M/H]$ scale (see Table 3) is considerably smaller than reported in Paper I and is now comparable to the corrections for the dwarf stars.

Figure 2 is a theoretical H-R diagram based on results from Paper I and this paper. Note the excellent match between the position of the giant branch and the isochrones, as well as an indication of an “edge” in the distribution of stars corresponding to the 1.8 Gyr isochrone. We will analyze this diagram in Paper III of this series for the complete sample.

5. CHROMOSPHERIC EMISSION

All of the spectra obtained for this project include the Ca II K and H lines and thus can be used to obtain measures of the chromospheric emission via emission reversals in the cores of these very strong lines. This is an important measurement, as chromospheric emission can be an indication of the age of a star and/or its binary status. An age determination can be important for exoplanet searches, especially for both the nulling-interferometer and coronagraphic designs of the *TPF*, because strong zodiacal light, scattered from a remnant protoplanetary disk, could mask weak planetary signals.

Paper I described in detail how we measure the chromospheric emission in our program stars. We follow the practice of the Mount Wilson chromospheric activity program (Baliunas et al. 1995) in measuring the fluxes in four bands; two of these bands, C_1 and C_2 , are continuum bands located just shortward and longward of the K and H lines, and the K and H bands are centered on the cores of the K and H lines (see Fig. 9 in Paper I). Our K and H bands are 4 Å wide, in contrast to the Mount Wilson 1 Å bandpasses, because of the lower resolution of our spectra.

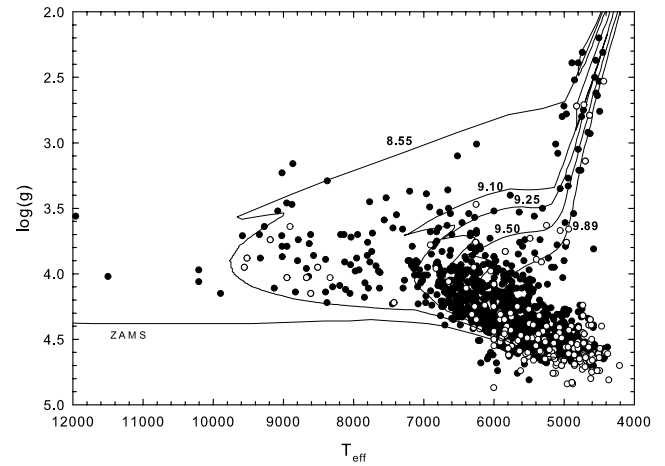


FIG. 2.—Astrophysical H-R diagram based on results reported in this paper and Paper I. The isochrones, included for illustrative purposes, are from Lejeune & Schaerer (2001). The isochrones are labeled with the logarithm of the age (8.55 = 350 million years, 9.10 = 1.3 Gyr, 9.25 = 1.8 Gyr, 9.50 = 3.5 Gyr, and 9.89 = 7.8 Gyr). The filled circles are for stars with $[M/H] > -0.40$, and open circles are for stars with $[M/H] < -0.40$.

The chromospheric emission index is calculated, like the Mount Wilson index, with the equation

$$S = 5 \frac{K + H}{C_1 + C_2}$$

Because the CTIO and SO spectra have different resolutions, there is a different instrumental system for each. The ultimate goal is to transform these instrumental systems onto the system of the Mount Wilson project, but to ensure homogeneity in the chromospheric indices reported in this series of papers we first transform these two instrumental systems to the DSO18 instrumental system established in Paper I. The DSO18 instrumental system (S_{18}) is then transformed to the Mount Wilson system (S_{MW}) using observations of a number of chromospheric activity “standards”—stars well observed by the Mount Wilson group and that, at least in their database ending in 1995, show no significant long-term secular trends (see Table 5 in Paper I). This transformation from S_{18} to S_{MW} was derived in Paper I.

To derive the transformations between S_{CTIO} and S_{18} and between S_{SO} and S_{18} we observed as many of the chromospheric “standard” stars mentioned in the above paragraph as possible from CTIO and SO. The resulting transformations are linear,

$$\begin{aligned} S_{18} &= 0.949 S_{\text{CTIO}} - 0.032, & \sigma &= 0.012, \\ S_{18} &= 0.904 S_{\text{SO}} + 0.002, & \sigma &= 0.011, \end{aligned}$$

and are illustrated in Figure 3.

As explained in Paper I, we have used the procedure of Noyes et al. (1984) to derive from S_{MW} the parameter $\log R'_{\text{HK}}$, which is a measure of the chromospheric flux in the cores of the K and H lines. This parameter may be used to classify stars into the chromospheric activity categories “very inactive” (VI), “inactive” (I), “active” (A), and “very active” (VA) (see Fig. 4). This parameter has been tabulated for stars in our sample with spectral types between F5 and M0 (see Table 2). However, the reader should bear in mind that the transformation from S_{MW} to $\log R'_{\text{HK}}$ becomes increasingly uncertain for stars with $B - V > 1.2$. In addition, this transformation is not well defined for $B - V < 0.5$. Thus, even though $\log R'_{\text{HK}}$ is tabulated in Table 2 for stars outside of this range, these values and the corresponding activity classifications

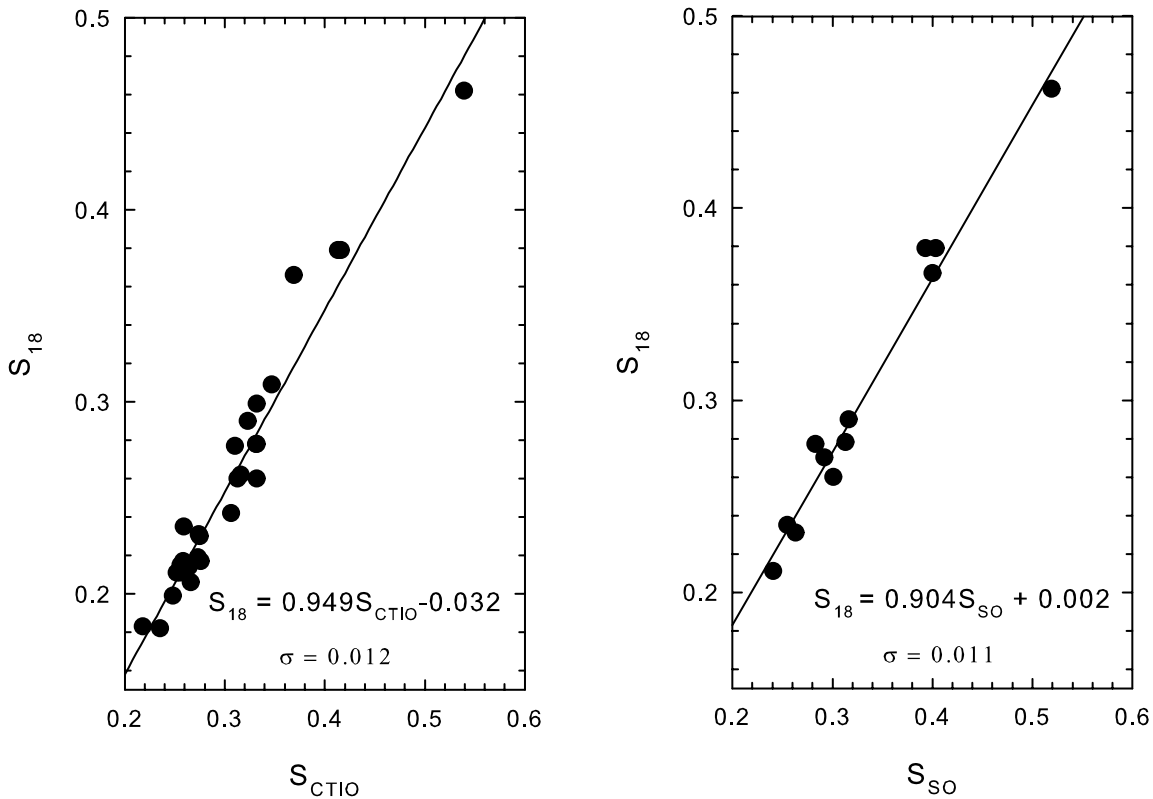


FIG. 3.—Transformations from the CTIO and SO chromospheric emission instrumental systems to the DSO18 instrumental system of Paper I.

should be treated with some caution. The distribution of this parameter with respect to metallicity is discussed in § 7.1, and that discussion is limited to stars with $0.5 < B - V < 1.2$.

A brief note on the relationship between our spectral classification notation for chromospheric activity (see § 3) and the classification into the activity classes VI, I, A, and VA afforded by the $\log R'_{\text{HK}}$ parameter is probably appropriate here. These two classification systems are generally in good agreement. For instance, nearly all of the “ke” and “kee” stars are either in the A or VA classes. However, the two systems are not redundant. The $\log R'_{\text{HK}}$ classification uses information external to the spectrum, in particular, the $B - V$ index and a model of the photospheric flux in the K line. It is also not defined for late K and early M dwarfs, nor does it contain any information about emission in the hydrogen lines. The

spectral classification notation, on the other hand, is self-sufficient; it may be used for M dwarfs, and it also contains information on Balmer-line emission, which is not necessarily well correlated with emission in Ca II K (see Thatcher & Robinson 1993).

6. NOTES ON ASTROPHYSICALLY INTERESTING STARS

HIP 3961 = HD 5028: We were somewhat surprised to find that this metal-weak F6 star turns out to be in the chromospherically very active category. However, visual inspection of the spectrum verifies that the Ca II K and H lines are both shallow. It turns out that this star is both an X-ray source (Haberl et al. 2000) and a far-UV source (Bowyer et al. 1995).

HIP 2235 = HD 2454: An F5 dwarf with an overabundance of strontium. Ba II $\lambda 4554$ also appears enhanced—see Tomkin et al. (1989).

HIP 16846 = HD 22468 = V711 Tau: This well-known RS CVn variable (of spectral type K2: Vn k) shows strong emission in Ca II K and H, with infilling in H β . The spectral lines appear broad.

HIP 29804 = HD 43848: This K2 subgiant shows a strong Swan band at 4737 Å.

HIP 30476 = HD 45289: From our spectral type, basic physical parameters, and chromospheric activity measurements, this star appears to be a very close solar twin (see § 7.2).

HIP 59750 = HD 106516: Both the SO and the CTIO spectra agree that this metal-weak F9 dwarf is a chromospherically active star. The CTIO spectrum, obtained on 2002 December 14, gives $\log(R'_{\text{HK}}) = -4.158$ (VA), and the SO spectrum, obtained on 2001 April 9, gives $\log(R'_{\text{HK}}) = -4.410$ (A). This star is an X-ray source and *may* have been the source of the 1993 January 13, gamma-ray burst—see Shibata et al. (1997).

HIP 64478 = HD 114630: The entire spectrum of this chromospherically active star (of spectral type G0 Vp k) appears

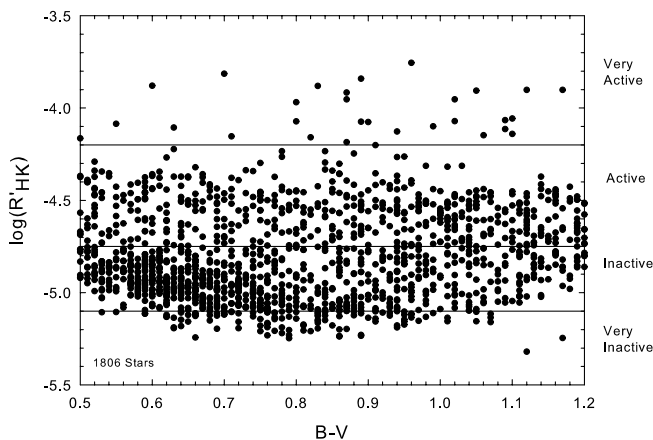


FIG. 4.—Chromospheric flux parameter $\log R'_{\text{HK}}$ vs. the $B - V$ color. This diagram allows the classification of stars into the chromospheric activity categories “very inactive,” “inactive,” “active,” and “very active.”

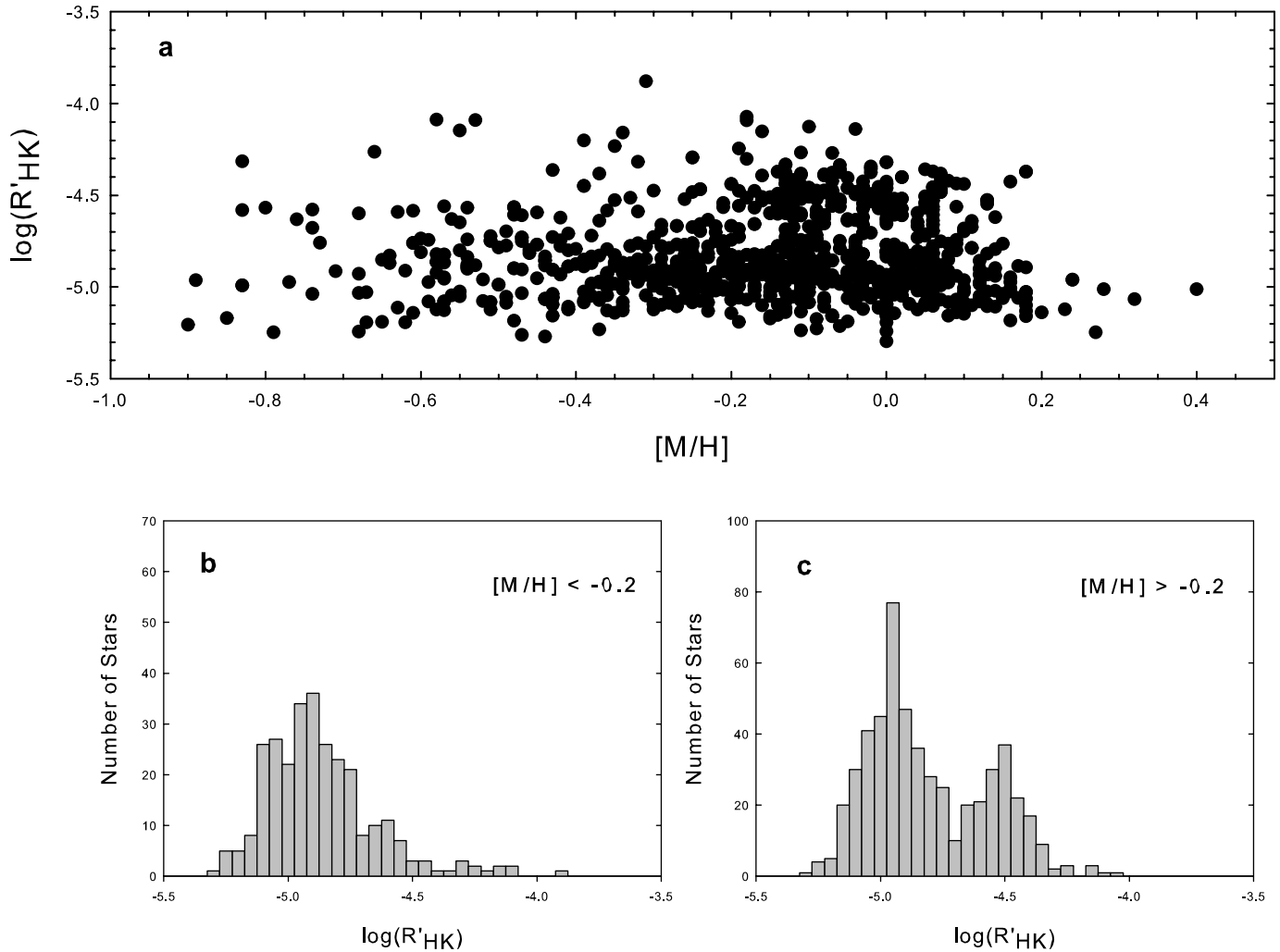


FIG. 5.—Distribution of the chromospheric activity parameter $\log R'_{\text{HK}}$ for dwarf F, G, and early K stars as a function of metallicity. In (a), activity increases along the vertical axis, while in (b) and (c) activity increases to the right. Panels (b) and (c) show histograms of the distribution of points in (a). Note that for stars with $[M/H] > -0.2$ the distribution is strongly bimodal, but it is single-peaked for $[M/H] < -0.2$. Also note that a tail of very active dwarf stars persists in the metal-weak distribution. Both of these points are discussed in § 7.1.

“veiled.” The resonance/low-excitation lines (such as $\text{Ca I } \lambda 4226$ and $\text{Fe I } \lambda 4046$) are particularly weak, the cores of Ca II K and H are shallow, and $\text{H}\beta$ appears slightly filled in. See a related discussion in § 7.1.

HIP 71908 = HD 128898: This well-known SrCrEu Ap star is also characterized by a broad Ca II K line.

HIP 76550: This star shows peculiar morphology in the 4780 Å MgH band (violet side weak), seen in both the CTIO and SO spectra.

HIP 96635 = HD 185181: This is a chromospherically active subgiant K2 star and thus a possible PMS star. Note that Koen & Eyer (2002) have found that this star is a variable from *Hipparcos* photometry but were unable to determine the type of variability.

HIP 98470 = HD 189245: This chromospherically very active late F-type star is an extreme ultraviolet source, a variable star, and a rapid rotator (86 km s^{-1}).

Also see notes on specific stars in § 7.1 and the notes to Table 2.

7. RESULTS AND DISCUSSION

7.1. Stellar Activity and $[M/H]$

In Paper I we demonstrated that the chromospheric emission parameter $\log R'_{\text{HK}}$ has a bimodal distribution (see Fig. 12 of

that paper). This is a manifestation of the well-known Vaughan-Preston gap (Vaughan & Preston 1980). However, it turns out that this bimodality is a strong function of metallicity (see Fig. 5); for stars with $[M/H] > -0.20$, the distribution is strongly bimodal (Fig. 5c), but the distribution is strictly single-peaked for stars of lower metallicity (Fig. 5b). This is perhaps not too surprising, as metal-weak stars will, on average, be older than metal-rich stars, and thus we should expect a smaller number of active metal-weak stars, but two things are remarkable: (1) the fact that there persists a tail of quite active stars even at quite low metallicities ($[M/H] \approx -0.50$) and (2) the sudden change to a single-peaked distribution at $[M/H] = -0.20$. We also note that the low-metallicity peak is somewhat shifted toward less negative values of $\log R'_{\text{HK}}$ (i.e., toward higher activity levels).

Let us consider this last point before we discuss points 1 and 2. The slight shift in the low-metallicity peak toward higher activity levels can be understood as a metallicity effect on the fluxes in the four bands used in the calculation of the chromospheric activity parameters S_{MW} and $\log R'_{\text{HK}}$ (see § 5). To illustrate this we have calculated both of these parameters using synthetic spectra with $T_{\text{eff}} = 5000 \text{ K}$ and $\log g = 4.5$ with $[M/H]$ ranging from -1.0 to 0.5 (see Table 4). Note that the activity class of these synthetic spectra (which do not include chromospheres)

TABLE 4
ACTIVITY CLASS AND METALLICITY

[M/H]	$B - V$	S_{MW}	$\log R'_{\text{HK}}$	AC
0.50.....	0.99	0.125	-5.279	VI
0.00.....	0.92	0.125	-5.245	VI
-0.50.....	0.87	0.134	-5.185	VI
-1.00.....	0.84	0.159	-5.054	I

NOTE.—VI represents the very inactive and I the inactive chromospheric activity classes (see text).

changes from VI for the metal-rich spectra to I for the metal-weak spectra. This suggests a need to update the procedure of Noyes et al. (1984) to calculate $\log R'_{\text{HK}}$ by including a correction factor for metallicity, but it also helps to explain the shift in the low-metallicity peak toward higher activity levels and the fact that only a few of the metal-weak stars in Table 2 have activity classes of VI. However, it does not help to explain the presence of an extended tail of very active stars visible in Figure 5*b*, which brings us back to point 1 above.

The nature of these “low-metallicity” chromospherically active stars may be explored by considering some examples.

HD 9054 = HIP 6856 = CC Phe is a chromospherically active K2 dwarf (K2+V k) with $\log R'_{\text{HK}} = -4.263$ (on the boundary between the A and VA categories). We have calculated $[M/H] = -0.66$. This star is a strong X-ray source, and Torres et al. (2000) have found that this star is a member of a very young nearby association, HorA, in the vicinity of the active star ER Eri. In this context the metal-weak nature of this star is very difficult to understand.

HD 146464 = HIP 79958 = V371 Nor is a very active K3 dwarf (K3 V ke) that is not well studied. Its position coincides closely with 1RXS J161915.7–553023, an X-ray source. Kinetically, this star appears to be a thin-disk star ($U, V, W = 3, 1, 1 \text{ km s}^{-1}$)—all kinematics quoted in this paper are heliocentric space velocities in a right-handed coordinate system with U pointing toward the Galactic center and are taken from Nordström et al. (2004)—but we have calculated $[M/H] = -0.55$.

Two BY Draconis variables from Paper I are also found to have low metallicities. These stars are as follows:

1. HD 45088 = HIP 30630 = OU Gem, which has a high-eccentricity orbit ($e = 0.15$) and the kinematics of a thin-disk star, $U, V, W = +9, -4, -11 \text{ km s}^{-1}$, but we found $[M/H] = -0.83$. Soderblom & Mayor (1993) list this star as a possible member of the UMa group (age $\approx 0.3 \text{ Gyr}$).

2. HD 218738 = HIP 114379 = KZ And, which also has the kinematics of a thin-disk star: $U, V, W = -8, -10, -3 \text{ km s}^{-1}$. We found $[M/H] = -0.53$.

These four stars are surprisingly metal-weak for active, low-velocity stars. Our metallicities for three of these four stars are in good agreement with those of the Geneva-Copenhagen group (Nordström et al. 2004), who base their metallicities on a calibration of the Strömgren m_1 index. Nordström et al. (2004) do not give a metallicity for HD 146464. Other less extreme examples may be found by examining Table 2. This observation, that many chromospherically active K dwarfs have “low” metal abundances, is not new. For instance, Rocha-Pinto & Maciel (1998) examined the $\log R'_{\text{HK}}$ index for a sample of G and K dwarfs and found that many of the most active stars had low values of the Strömgren m_1 index, which measures line blanketing in the violet part of the spectrum. Giampapa et al. (1979) observed solar active and quiescent regions with the Strömgren *uvby* system and

found that the solar active regions are up to 35% more metal deficient than the quiescent regions based on the m_1 index. Favata et al. (1997) also demonstrated the depression of the m_1 index for active K stars but obtained red spectra for a number of these stars and showed that these spectra gave normal (roughly solar) abundances. They suggested that the depression of the m_1 index is due to emission or infilling of the H δ line, which lies in the Strömgren v band. However, a careful examination of the spectra of our four low-metallicity active K dwarfs does not show emission or even infilling of the H δ line (at least in ratio with nearby metallic lines), with the possible exception of HD 146464, which may show a slight infilling of the H δ line. On the other hand, all of these stars show a marked weakening of the line spectrum in the blue-violet region (up to at least 4400 Å) relative to solar-abundance chromospherically inactive stars of the same spectral types, which are easily apparent even on visual inspection (we did not use the MK K-dwarf standards for this comparison, as some of these standards are metal-weak, while others are chromospherically active and may show some veiling themselves). The veiling seems most pronounced in the Ca I $\lambda 4226$ line and in the vicinity of the CN 0, 1 band with a band head at 4216 Å. Basri et al. (1989), using high-resolution spectra, have shown that the equivalent width of metallic lines in the blue-violet region can be reduced in highly active stars, which correlates well with what we see in our blue-violet spectra. Whether this infilling of the metallic lines is due to line emission or continuum emission is not clear at this point, but this phenomenon does seem to be the best explanation for the observed metallicity effect.

We note, however, that there are a few very active K dwarfs in our sample that do not seem to show a pronounced metallicity effect. For instance, HD 26354 (AG Dor), HD 111038 (LO Mus), and HD 220140 (V368 Cep) have K-line emission and $\log R'_{\text{HK}}$ indices that place them in the very active category but have, according to our determinations, metallicities that are only slightly subsolar. Both HD 26354 and HD 220140 have been classified as RS CVn binaries. LO Mus is not well studied but appears to be a BY Draconis star (Kazarovets et al. 1999). Other less extreme examples can be found in Table 2. HD 26354 does not show any veiling and even has a slightly stronger CN band than normal K2 solar-metallicity dwarfs (its gravity, however, is consistent with it being a dwarf and not a subgiant). HD 220140 also has a gravity consistent with a dwarf classification. HD 111038 shows marginal veiling, and HD 220140 shows some veiling, especially in the far violet (just longward of the K and H lines) and in Ca I $\lambda 4226$, which also appears slightly weak in HD 111038. To add to the mystery, however, the Geneva-Copenhagen group (Nordström et al. 2004) find, from their calibration of the Strömgren m_1 index, that these three stars are quite metal-weak.

It is difficult to understand why some of these very active K dwarfs show a pronounced metallicity effect and veiling and others do not. Both groups contain active binary stars and both contain objects that are *Extreme Ultraviolet Explorer* and X-ray sources. We speculate, however, that the chromospheres of these two groups may differ significantly. For instance, the “veiling” effect that is more prevalent in the metallicity-effect stars is largely seen in resonance or low-excitation lines of neutral metals in the violet region of the spectrum, such as Ca I $\lambda 4226$. The cores of such lines are formed in the temperature minimum region, whereas the emission reversals in the Ca II K and H lines are formed higher in the chromosphere in G and K dwarfs. This may mean that the temperature structure and/or the density in the temperature minimum region is different in the metallicity-effect active K dwarfs. Additional observations, to quantify and

TABLE 5
SOLAR ANALOGS

HIP	HD	Notes
699.....	361	*
1444.....	1388	D
1954.....	2071	*D
3578.....	4392	
6455.....	8406	*

NOTES.—Table 5 is published in its entirety in the electronic edition of the *Astronomical Journal*. A portion is shown here for guidance regarding its form and content. Symbols in the notes column have the following meanings: asterisks indicate a solar analog with spectral type within 1 subclass of the Sun; double asterisks indicate a candidate solar twin with spectral type and physical parameters very similar to those of the Sun; D indicates a star that is already in the Keck, Lick, and AAT Doppler planet-search program (see Valenti & Fischer 2005); and EP indicates a star with a known exoplanet.

to determine the nature of the infilling of the metallic-line spectrum in the metallicity-effect objects, will be required to resolve this question.

We now consider point 2. The sudden change from bimodality to single-peaked behavior at $[M/H] = -0.2$ becomes even more pronounced when the metallicity effects discussed in the above paragraphs are taken into account because many (although not all) of the active “low-metallicity” dwarfs in the high-activity tail in the $[M/H] < -0.2$ distribution really belong at $[M/H] > -0.2$. Two possible exceptions are HD 9770, an active triple (quintuple?) system that has kinematics typical of an old disk star (see Eggen 1962; Watson et al. 2001), and BF Lyn, a BY Dra variable with kinematics (U , V , $W = -22$, -51 , -28 km s^{-1}) suggestive of a thick-disk star. This sharp transition from bimodality to single-peaked behavior at $[M/H] = -0.2$ suggests that the cause of this phenomenon is not primarily age-related but rather is associated with some parameter necessary for the generation of an active chromosphere that is switched off at this divide. We expect that this parameter has something to do with rotation or, more specifically, differential rotation, but we do not have sufficient data to speculate further.

7.2. Solar Analogs

In Table 5 we have, for the benefit of users who are interested in solar analogs and twins and exoplanet searches, extracted from Table 2 all those dwarf stars (a total of 61) that satisfy the following requirements: (1) spectral types between G0 and G5, (2) $\log g > 4.20$, (3) $[M/H] > -0.10$, and (4) be single or members of wide doubles. In this table we have further distinguished those stars that have spectral types, basic physical parameters, and activity levels that are close (*) and very close (**) to those of the Sun. Indeed, those marked ** in the table can be considered solar twin candidates. We have also indicated in this table those that have known exoplanets and those that are currently on the Keck, Lick, and AAT Doppler planet-search program, according to Valenti & Fischer (2005).

7.3. Metallicity Distribution of the Solar Neighborhood

Information regarding the star formation and the chemical enrichment history of the Galactic disk can be derived from the metallicity distribution of the solar neighborhood. We have used data in Table 2 of this paper and Table 1 of Paper I to plot a

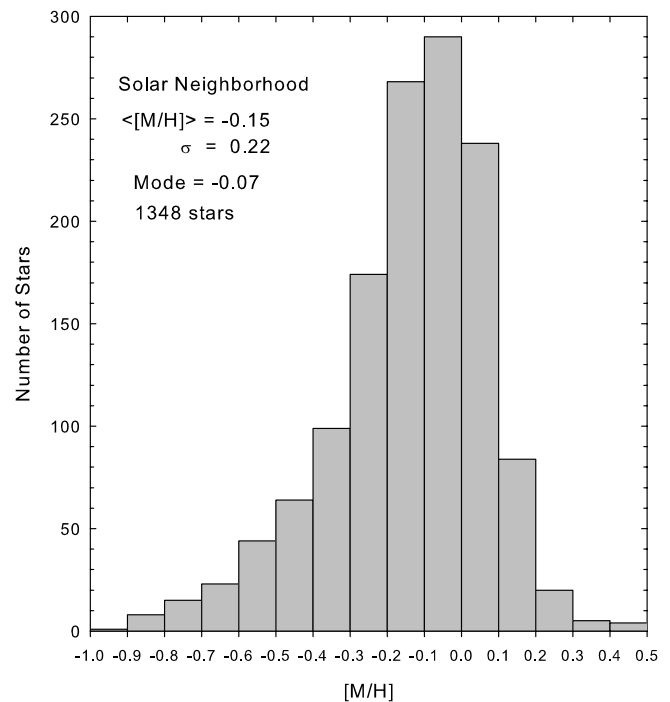


FIG. 6.—Histogram of the metallicity distribution for stars in our sample in the solar neighborhood. Note the extended low-metallicity tail, composed mostly of stars from the thick disk.

histogram of $[M/H]$ for our sample of stars. This histogram, based on 1348 stars, appears in Figure 6.

It is clear that this distribution is basically Gaussian with an enhanced low-metallicity tail, probably due to thick-disk stars, some “metallicity-effect” active K stars (see § 7.1), and even a few interloping halo stars (our sample, for instance, includes HD 19445, a well-studied halo star with $[Fe/H] \approx -2$). Taking a straight mean, we find $\langle [M/H] \rangle = -0.15$ with a dispersion of 0.22 dex. This is in excellent agreement with the recent determination by the Geneva-Copenhagen survey (Nordström et al. 2004; -0.14 , $\sigma = 0.19$) and is also similar to one found for K-type giants by Girardi & Salaris (2001).

However, if one is interested in the metallicity distribution of the thin-disk population, thick-disk and halo stars in the low-metallicity tail must be removed by reference to kinematics. We will carry out this analysis in Paper III, where we will publish results for the remainder of our sample, but it is clear that the result will be close to the *mode* of the present distribution, i.e., $[M/H] = -0.07$, which is very similar to the result of Luck & Heiter (2005), who found $\langle [Fe/H] \rangle = -0.04$ for a sample of 114 thin-disk stars within 15 pc of the Sun.

8. CONCLUDING REMARKS

We have presented results for 1676 dwarf and giant stars within 40 pc of the Sun including new, homogeneous spectral types, basic physical parameters, and measures of chromospheric activity. We will complete our study of the dwarf and giant stars earlier than M0 within 40 pc in the third and final paper of this series. The goals of this project are to characterize the stellar population in the solar neighborhood and to provide data that will be useful in the selection of targets for the *Space Interferometry Mission* and the *Terrestrial Planet Finder* mission. The data presented in this paper are currently available on the project’s Web site, and work is continuing on the remaining stars in the project.

This work has been carried out under contract with NASA/JPL (JPL contract 526270) and has been partially supported by grants from the Vatican Observatory and Appalachian State University. This research made use of the SIMBAD database, operated at CDS, Strasbourg, France. We would also like to thank Jean-Claude Mermilliod for his assistance in the compilation of photometry

for our database and his maintenance (with M. Mermilliod) of the Web-based General Catalogue of Photometric Data (Mermilliod et al. 1997), which has proved very useful in this research. Many thanks to Kelly Kluttz and Chris Jackolski, both of Appalachian State University, for help in various aspects of this project.

REFERENCES

- Allende Prieto, C., Barklem, P. S., Lambert, D. L., & Cunha, K. 2004, *A&A*, 420, 183
- Alonso, A., Arribas, S., & Martínez-Roger, C. 1996, *A&A*, 313, 873
- . 1999, *A&AS*, 140, 261
- Baliunas, S. L., et al. 1995, *ApJ*, 438, 269
- Basri, G., Wilcots, E., & Stout, N. 1989, *PASP*, 101, 528
- Blackwell, D. E., & Lynas-Gray, A. E. 1994, *A&A*, 282, 899
- Bowyer, S., Sasseen, T. P., Wu, X., & Lampton, M. 1995, *ApJS*, 96, 461
- Cayrel de Strobel, G., Soubiran, C., & Ralite, N. 2001, *A&A*, 373, 159
- Eggen, O. J. 1962, *R. Obs. Bull.*, 51
- Favata, F., Micela, G., Sciortino, S., & Morale, F. 1997, *A&A*, 324, 998
- Garrison, R. F. 1994, in *ASP Conf. Ser. 60, The MK Process at 50 Years*, ed. C. J. Corbally, R. O. Gray, & R. F. Garrison (San Francisco: ASP), 3
- Giampapa, M. S., Worden, S. P., & Gilliam, L. B. 1979, *ApJ*, 229, 1143
- Girardi, L., & Salaris, M. 2001, *MNRAS*, 323, 109
- Gorda, S. Yu., & Svechnikov, M. A. 1998, *Astron. Rep.*, 42, 793
- Gray, R. O. 1989, *AJ*, 98, 1049
- Gray, R. O., & Corbally, C. J. 1994, *AJ*, 107, 742
- Gray, R. O., Corbally, C. J., Garrison, R. F., McFadden, M. T., & Robinson, P. E. 2003, *AJ*, 126, 2048 (Paper I)
- Haberl, F., Filipović, M. D., Pietsch, W., & Kahabka, P. 2000, *A&AS*, 142, 41
- Hamuy, M., Walker, A. R., Suntzeff, N. B., Gigoux, P., Heathcote, S. R., & Phillips, M. M. 1992, *PASP*, 104, 533
- Henry, T. J., Walkowicz, L. M., Barto, T. C., & Golimowski, D. A. 2002, *AJ*, 123, 2002
- Kazarovets, A. V., Samus, N. N., Durlevich, O. V., Frolov, M. S., Antipin, S. V., Kireeva, N. N., & Pastukhova, E. N. 1999, *Inf. Bull. Variable Stars*, 4659, 1
- Keenan, P. C. 1984, in *The MK Process and Stellar Classification*, ed. R. F. Garrison (Toronto: DDO), 20
- Keenan, P. C., & McNeil, R. C. 1989, *ApJS*, 71, 245
- Koen, C., & Eyer, L. 2002, *MNRAS*, 331, 45
- Kurucz, R. L. 1993, *Kurucz CD-ROM 13, ATLAS9 Stellar Atmosphere Programs and 2 km s⁻¹ Grid* (Cambridge: SAO)
- Lejeune, T., & Schaerer, D. 2001, *A&A*, 366, 538
- Luck, R. E., & Heiter, U. 2005, *AJ*, 129, 1063
- Makarov, V. V., & Kaplan, G. H. 2005, *AJ*, 129, 2420
- Mermilliod, J.-C., Mermilliod, M., & Hauck, B. 1997, *A&AS*, 124, 349
- Nordström, B., et al. 2004, *A&A*, 418, 989
- Noyes, R. W., Hartmann, L. W., Baliunas, S. L., Duncan, D. K., & Vaughan, A. H. 1984, *ApJ*, 279, 763
- Perryman, M. A. C. et al. 1997, *The Hipparcos and Tycho Catalogues* (ESA SP-1200; Noordwijk: ESA)
- Press, W. H., Teukolsky, S. A., Vetterling, W. T., & Flannery, B. P. 1992, *Numerical Recipes in C* (2nd ed.; Cambridge: Cambridge Univ. Press)
- Rocha-Pinto, H. J., & Maciel, W. J. 1998, *A&A*, 339, 791
- Shibata, R., Murakami, T., Ueda, Y., Yoshida, A., Tokanai, F., Otani, C., Kawai, N., & Hurley, K. 1997, *ApJ*, 486, 938
- Sinachopoulos, D. 1989, *A&AS*, 81, 103
- Soderblom, D. R., & Mayor, M. 1993, *AJ*, 105, 226
- Thatcher, J. D., & Robinson, R. D. 1993, *MNRAS*, 262, 1
- Tomkin, J., Lambert, D. L., Edvardsson, B., Gustafsson, B., & Nissen, P. E. 1989, *A&A*, 219, L15
- Torres, C. A. O., Da Silva, L., Quast, G. R., De La Reza, R., & Jilinski, E. 2000, *AJ*, 120, 1410
- Valenti, J. A., & Fischer, D. A. 2005, *ApJS*, 159, 141
- Vaughan, A. H., & Preston, G. W. 1980, *PASP*, 92, 385
- Watson, L. C., Pritchard, J. D., Hearnshaw, P. M., & Gilmore, A. C. 2001, *MNRAS*, 325, 143